



Full paper/Mémoire

Diesel soot oxidation by nitrogen dioxide, oxygen and water under engine exhaust conditions: Kinetics data related to the reaction mechanism[☆]

Nabila Zouaoui^a, Madona Labaki^b, Mejdi Jeguirim^{a,*}^a Institut de science des matériaux de Mulhouse, université de Haute-Alsace, 15, rue Jean-Starcky, BP 2488, 68057 Mulhouse, France^b Laboratory of Physical Chemistry of Materials (LPCM)/PR2N, Faculty of Sciences II, Lebanese University, Fanar, P.O. Box 90656, Jdeidet El-Metn, Lebanon

ARTICLE INFO

Article history:

Received 14 May 2013

Accepted after revision 9 September 2013

Available online 13 December 2013

Keywords:

Kinetic constants

Reaction mechanism

Soot oxidation

ABSTRACT

Experimental studies on diesel soot oxidation under a wide range of conditions relevant for modern diesel engine exhaust and continuously regenerating particle trap were performed. Hence, reactivity tests were carried out in a fixed bed reactor for various temperatures and different concentrations of oxygen, NO₂ and water (300–600 °C, 0–10% O₂, 0–600 ppm NO₂, 0–10% H₂O). The soot oxidation rate was determined by measuring the concentration of CO and CO₂ product gases. The parametric study shows that the overall oxidation process can be described by three parallel reactions: a direct C–NO₂ reaction, a direct C–O₂ reaction and a cooperative C–NO₂–O₂ reaction. C–NO₂ and C–NO₂–O₂ are the main reactions for soot oxidation between 300 and 450 °C. Water vapour acts as a catalyst on the direct C–NO₂ reaction. This catalytic effect decreases with the increase of temperature until 450 °C. Above 450 °C, the direct C–O₂ reaction contributes to the global soot oxidation rate. Water vapour has also a catalytic effect on the direct C–O₂ reaction between 450 °C and 600 °C. Above 600 °C, the direct C–O₂ reaction is the only main reaction for soot oxidation. Taking into account the established reaction mechanism, a one-dimensional model of soot oxidation was proposed. The roles of NO₂, O₂ and H₂O were considered and the kinetic constants were obtained. The suggested kinetic model may be useful for simulating the behaviour of a diesel particulate filter system during the regeneration process.

© 2013 Académie des sciences. Published by Elsevier Masson SAS. All rights reserved.

R É S U M É

Mots clés :

Constantes cinétiques

Mécanisme réactionnel

Oxydation des suies

Une étude expérimentale sur l'oxydation des suies diesel a été menée dans des conditions opératoires proches du fonctionnement des échappements Diesel et de la régénération continue des filtres à particules. Les tests de réactivité ont été effectués dans un réacteur à lit fixe pour différentes températures et concentrations d'oxygène, de NO₂ et de vapeur d'eau (300–600 °C, 0–10 % O₂, 0–600 ppm NO₂, 0–10 % H₂O). La vitesse d'oxydation des suies a été déterminée à partir des concentrations des espèces CO et de CO₂ formées. L'étude paramétrique montre que l'oxydation des suies par un mélange gazeux contenant NO₂, O₂ et H₂O peut être décrite par trois réactions d'oxydation distinctes : une réaction directe C–NO₂, une réaction directe C–O₂ et une réaction coopérative C–NO₂–O₂. Les

[☆] Thematic issue devoted to François Garin.

* Corresponding author.

E-mail address: mejdi.jeguirim@uha.fr (M. Jeguirim).

réactions C–NO₂ et C–NO₂–O₂ sont les principales réactions d'oxydation des suies se déroulant entre 300 et 450 °C. La vapeur d'eau agit comme un catalyseur sur la réaction directe C–NO₂. Cet effet catalytique diminue avec l'augmentation de la température jusqu'à 450 °C. Au-dessus de 450 °C, la réaction directe C–O₂ contribue à la vitesse globale d'oxydation des suies. La vapeur d'eau exerce également un effet catalytique sur la réaction directe C–O₂ pour des températures comprises entre 450 °C et 600 °C. À partir de 600 °C, la réaction directe C–O₂ est la seule réaction responsable de l'oxydation des suies. À partir du mécanisme réactionnel obtenu, un modèle monodimensionnel de l'oxydation des suies a été établi. Les rôles de NO₂, O₂ et H₂O ont été pris en compte et les constantes cinétiques ont été obtenues. Le modèle cinétique établi peut être utile pour simuler le comportement d'un système de filtre à particules diesel pendant le processus de régénération.

© 2013 Académie des sciences. Publié par Elsevier Masson SAS. Tous droits réservés.

1. Introduction

The improved performance and the low specific fuel consumption of diesel engines caused an increasing demand, during the last years, of cars powered by diesel engines. However, diesel engines produce NO_x and particles of carbonaceous soot (PM), which consist of unburned organic compounds and other solid and liquid material. NO_x and particulates from diesel engines have been identified to generate harmful effects on human health and the environment. To satisfy European and US regulations, extensive efforts have been focused on how to reduce emissions of pollutants, by controlling the combustion process and by developing efficient after-treatment systems. Currently, diesel particulate filters (DPF) are considered very effective a solution to attain the particulate matter (PM) emission standards since they have proved to meet serious diesel engine pollution reduction limits with filtration efficiencies exceeding 90 %. However, soot retained from exhaust gases should be removed to prevent back pressure and therefore a DPF regeneration is necessary. In the diesel exhaust emissions, NO₂ and O₂ are the main oxidants in presence. Hence, soot oxidation by these oxidants is an alternative to regenerate the filters. Several studies focused on the investigation of the uncatalyzed and catalyzed soot oxidation reaction by O₂ and/or NO₂ in the presence or absence of H₂O. Many mathematical models were proposed to simulate these processes in order to understand thoroughly the inherent mechanisms, to predict the behaviour of DPF during its usage and to contribute to the improvement of the design process. Jeguirim et al. [1] studied the adsorption and reduction of NO₂ at low temperatures (50 °C) on activated carbon and evidenced the formation of surface complexes such as –C(ONO₂), –C(NO₂) and –C(O). Gao et al. [2] found similar results. Muckenhuber and Grothe [3] proposed a reaction mechanism where two oxygen atoms from two different NO₂ molecules are transferred onto the carbon surface. In this case, NO₂ reacts directly with the carbon surface to form an acidic functional group, of acyl-nitrite type, as intermediate only. Du et al. [4] studied the oxidation by oxygen of uncatalyzed and calcium-catalyzed soot by means of Thermogravimetric Analysis (TGA) and Temperature-Programmed Desorption (TPD). They concluded that the products of the reaction, CO and CO₂, are generated via different mechanisms and that CO₂ was

formed on sites different from CO ones. They formulated a model where the carbon structure is the controlling factor for the uncatalyzed oxidation and where calcium dispersion on the carbon surface is that for the catalyzed reaction. He et al. [5] simulated the CO/CO₂ ratio obtained during char combustion by taking into account the pore model, the gas diffusion inside the pores and the reaction between carbon and oxygen. They concluded that the secondary reactions and pore structure significantly influenced the CO/CO₂ ratio. Biggs and Agarwal [6] investigated the ratio CO/CO₂ on a porous char particle in a fluidized bed and suggested a relationship between the CO/CO₂ ratio and the char particle size. Floess et al. [7] found that the reactivity of char is a function of particle size for particles between 50 and 200 μm in diameter. This effect is not observed for macroporous char networks. Neef et al. [8] studied the kinetics of the uncatalyzed oxidation, in oxygen/argon atmosphere with or without water, of two types of soot: flame soot (Printex U) and diesel soot, in the temperature range 450–550 °C in a flow reactor. A kinetic model, taking into account the conversion factor, was proposed and discussed. Jacquot et al. [9] and Jeguirim et al. [10–12] studied the kinetics of the reaction between NO₂ and carbon in the presence of O₂ and H₂O in a fixed bed reactor. The rate increase of carbon consumption by NO₂ in the presence of O₂ was attributed to the reaction between NO₂ and the intermediate species formed by the adsorption of oxygen on the carbon surface. Water presence increases the rate of carbon consumption because of the formation of intermediate nitric and nitrous acids which enhance the rate of C–NO₂ reaction. However, the oxygen of water is not consumed and thus water is considered as a catalyst for the carbon oxidation reaction [12]. A monodimensional model was developed and kinetic parameters were extracted for the temperature range 300–400 °C [9–11]. Carbon oxidation by O₂–NO₂–H₂O in a flow reactor was also studied at 250–500 °C by Jung et al. [13] who proposed reaction mechanisms and extracted kinetic constants. Schejbal et al. [14] developed a model for the soot deposition on the DPF and its regeneration based on the detailed kinetics of catalyzed and uncatalyzed soot combustion by O₂ and NO₂ developed by Jeguirim et al. [12]. The role of NO₂ and O₂ in the combustion of soot was also investigated by Setiabudi et al. [15] on three kinds of soot in the temperature range 100–450 °C in a flow reactor system and by thermogravimetry. The intermediates of

soot oxidation were studied by infrared spectroscopy. Tighe et al. [16] studied the kinetics of oxidation by NO_2 of three types of soot from a diesel engine in a packed bed at various temperatures (300–550 °C). The kinetics of the oxidation of four types of model and real diesel soot, by NO_2 and O_2 , with or without water, in a flat bed reactor was also studied by Messerer et al. [17], who proposed a kinetic model to simulate experimental results. Kinetic data concerning the reaction between soot and NO_2 have been also obtained by Kleffmann et al. [18], Arens et al. [19], Keil et al. [20], Prince et al. [21], Lur'e and Mikhno [22], Gray and Do [23] and Leistner et al. [24]. A theoretical study of the interaction between soot and NO in the absence of oxygen was carried out by Raj et al. [25] in order to develop the mechanistic understanding behind the formation of chemical species such as CO, N_2 and N_2O on soot. The energetics and kinetics were respectively evaluated using density functional theory and transition state theory. The model predicted well the formation of CO at temperatures > 600 °C using the rate observed experimentally in soot-NO environments. López-Fonseca et al. [26] established a kinetic model for the oxidation by oxygen of two diesel soot-like materials in a thermobalance (dynamic thermogravimetry). In the model established by these authors, the conversion factor was taken into consideration. Zouaoui et al. [27] proposed experimental and theoretical procedures to extract kinetic constants for the C– O_2 reaction, taking into account oxygen diffusivity, from thermogravimetric experiments, in the temperature range 550–700 °C. Similar studies were carried out on soot and Printex U by Kalogirou and Samaras [28] and on two types of soot by Song et al. [29]. The catalytic combustion of carbon or soot by oxygen and/or NO_2 has also received much attention [4,11,14,30–36]. Several kinetics data based on the catalytic mechanism were available.

The analysis of these literature data shows that most proposed models do not cover the whole temperature range 300–600 °C. Furthermore, there is a lack of data on the influence of the different components of diesel exhausts (O_2 , NO_2 , H_2O) at different temperatures. It should also be added that the modification of the structure and physical properties of carbon or soot during the combustion process is well known in the literature but few simulation studies [4,7,8,16,17,26] took into consideration in their proposed models the variation of the kinetic rate of isothermal soot combustion with the conversion of soot mass, which is a consequence of the carbon structure variation. A recent investigation has used thermogravimetric analysis to propose a detailed set of kinetic reactions for soot oxidation by simulating diesel exhaust emissions but without investigating the effect of water vapour presence [37]. Hence, a detailed kinetic model for soot oxidation under real diesel engines conditions (NO_2 – O_2 – H_2O) in a wide temperature range, 300–600 °C, where the influence of each gaseous species present is clearly taken into account and where the evolution of kinetic constants in isothermal conditions is considered, is necessary for car manufacturers and industrialists since simulation models can offer an important contribution to the improvement of the design process of diesel engines.

The objective of the present work is to perform experimental studies on carbon – taken as diesel soot model – combustion in conditions close to real diesel emissions, to study the influence of some main oxidants present in the real atmosphere of diesel engines (O_2 , NO_x , H_2O) at different temperatures (300–600 °C) and mixture compositions and then to elaborate a detailed kinetic model. Experimental studies will be carried out in a fixed bed reactor under a continuous flow of gases to mimic real diesel exhaust conditions.

2. Experimental part

The activity for soot oxidation was determined using commercially available carbon black powders Vulcan 6 (95.3 % C, 2.1 % O, 0.7 % H, 1 % S, and 0.3 % N). The use of this commercial soot for laboratory studies is chosen as it can be obtained in large quantities with reproducible characteristics unlike diesel soot.

Isothermal oxidation tests were carried out in a fixed-bed reactor (FBR) in a large range of temperatures (300–600 °C) and various oxygen, NO_x and water concentrations (0–10 % O_2 , 0–600 ppm NO_2 , 0–10 % H_2O). NO, very present in the diesel exhaust, is not discussed in this study since NO does not oxidize directly soot. Moreover, the role of NO on soot oxidation was only observed in the presence of catalyst and O_2 [38]. The description of the FBR and the experimental procedure were reported elsewhere [9,10]. In each experiment, 10–50 mg of carbon black (CB) were used. The total flow rate was fixed to 100 $\text{NL}\cdot\text{h}^{-1}$ at 1 atm. The molar fractions of NO_2 , NO, CO_2 and CO in the reactor exhaust were continuously measured by a UV absorption analyzer (Rosemount NGA 2000, Germany) and an infrared unit (MaihacMultor 610, France). Table 1 summarizes all the experimental conditions tested in this study.

The gas–solid reaction may occur in the diffusion and/or kinetic regime. To ensure that all the experiments reported here were not affected by such limitations, a series of experiments with various CB mass (10–50 mg, 100 mg and 200 mg) and flow rate (50 $\text{NL}\cdot\text{h}^{-1}$, 75 $\text{NL}\cdot\text{h}^{-1}$ and 100 $\text{NL}\cdot\text{h}^{-1}$) were previously examined [11,27]. No significant effect of the initial soot mass and of the flow rate on the specific rate of the soot oxidation was observed [11]. Moreover, it was checked that no significant exothermicity occurred during our isothermal runs. Heat limitations are negligible under our experimental conditions [27].

3. Results and discussions

Fig. 1 shows a typical temporal evolution of CO, CO_2 , NO and NO_2 emissions in the FBR outlet during soot oxidation experiments (10 mg CB, 400 ppm NO_2 , 10 % O_2 , 5 % H_2O ,

Table 1
Summary of our operating conditions.

Temperatures (°C)	300, 350, 400, 450, 500, 550, 600
NO_2 (ppm)	200, 400, 600
O_2 (%)	0, 2, 5, 10
H_2O (%)	0, 2, 5, 10
Flow ($\text{NL}\cdot\text{h}^{-1}$)	100
Mass of CB (mg)	10–25–50

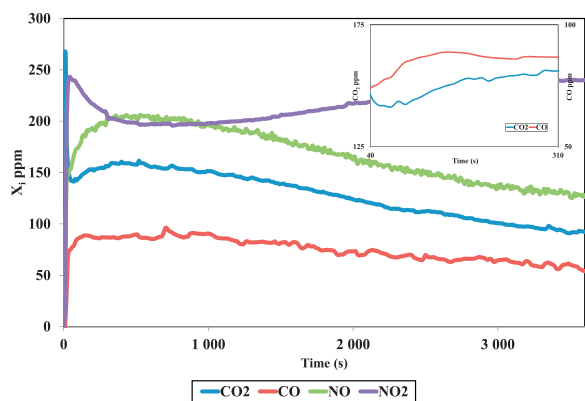


Fig. 1. (Colour online) Outlet concentrations of CO₂, CO, NO and NO₂ versus time at 500 °C.

500 °C). Oxygen and water are not reported in the figure because they are in excess. For this reaction, emission curves of CO, CO₂ and NO have similar shapes. These compounds are linked to the same oxidation mechanism.

At the beginning of combustion, during 300 s, CO and CO₂ concentration increases with time (Cf. the subfigure in Fig. 1) indicating an increase of the oxidation rate. The increase of the oxidation rate during the first 300 s is also observed for the various experimental conditions. In addition, the trend of CO and CO₂ was similar during the first seconds for the different experimental tests and the ratio CO₂/CO was almost constant for a conversion percentage lower than 10%. However, the CO₂/CO values depend strongly on the gas inlet composition and temperature. This point is discussed further in the oxidation mechanism section.

After 300 s, CO and CO₂ concentrations decrease with time. The increase of the combustion rate, during the first stage of combustion, was explained by several hypotheses. Jeguirim et al. attributed this first step to the formation of nitrogen species on the carbon surface [10]. Zouaoui et al. attributed the increase of the oxidation rate to an increase of the specific surface area of CB [27]. Indeed, they measured the specific surface area of CB, by the BET method, at different stages of CB combustion (for different conversion percentages). They found an increase in the specific surface area of the carbonaceous material with the increase of CB conversion up to 50 %.

Fig. 1 shows also that when the NO₂ was turned on, it reacted with the soot, producing a peak in NO. The NO₂ was also detected during the reaction, thus not all NO₂ reacted with the soot. Nitrogen balance analysis confirms that NO and NO₂ are the only nitrogenous species emitted during soot oxidation.

In order to identify the effect of operating conditions (gas composition, temperature), oxidation rates were compared at a fixed conversion percentage for the different experimental situations. The specific oxidation rate was calculated from the total gas flow rate and the CO and CO₂ emissions using the following equation:

$$-\frac{1}{m_i} \frac{dm}{dt} = (X_{CO} + X_{CO_2}) \times F \times M_C \quad (1)$$

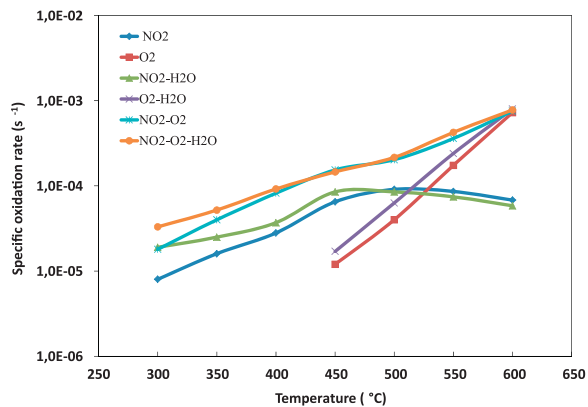


Fig. 2. (Colour online) Influence of the inlet gas composition on the specific soot oxidation rate for 10 % soot conversion.

where X_{CO} and X_{CO_2} are the measured molar fractions of CO and CO₂ in the gas phase, F is the molar flow of gases through the reactor, m_i and M_C are the initial and the molar mass of carbon, respectively.

Fig. 2 shows the specific oxidation rate versus inlet gas composition and temperature for a soot conversion rate of 10 %. Fig. 2 shows that the direct oxidation of soot by NO₂ starts at the low temperatures (~ 300 °C). The oxidation rate is enhanced by the presence of O₂ through the formation of C(O) complexes decomposed by NO₂. Above 450 °C, the direct oxidation of soot by O₂ starts and becomes the dominant reaction above 600 °C. Water vapour has a beneficial effect on the direct C–NO₂ and C–O₂ reactions. This beneficial effect decreases with temperature.

In order to assess further the role of each component on the reaction mechanism of soot oxidation, several calculations were performed. Hence, to get some information about the participation of H₂O in the C–NO₂ reaction, the oxygen contribution from oxygenated species NO₂ and H₂O was estimated [12]. These calculations show that the oxygen of water is not consumed and thus water is considered as a catalyst for the oxidation reaction of carbon [12]. This catalytic effect was attributed to the formation of intermediate nitric and nitrous acids which enhance the rate of C–NO₂ reaction [10].

The beneficial effect of water vapour on the direct C–O₂ reaction was also analysed. Hence, experimental tests of direct oxidation of carbon by water vapour were performed at the 450–600 °C temperature range. During, these tests, no significant oxidation of CB occurred. Therefore, the beneficial effect of water may be attributed to a catalytic effect. Such behaviour was mentioned previously by Ahlström and Odenbrand [43].

The evolution of the CO₂/CO ratio was also examined for different experimental conditions. It was shown that the CO₂/CO ratio decreases from 5 at 300 °C to 2.3 at 450 °C for the direct C–NO₂ reaction. The values in the presence of water vapour are higher than those in the absence of water ranging from 6 to 2.7 between 300 and 450 °C.

The evolution of the CO₂/CO ratio during the direct C–O₂ reaction in the absence and in the presence of water vapour was assessed. It was observed that the CO₂/CO ratio

decreases from 1.6 to 0.8 in the absence of water and from 2 to 0.95 in the presence of water between 500 and 600 °C for a conversion percentage of 20 %. It was also observed that the CO₂/CO ratio decreases in the absence of water with time until a conversion percentage of 50 %. In contrast, the CO₂/CO ratio increases in the presence of water with time until a conversion percentage of 50 %. These observations may confirm the beneficial effect of water on the direct C–O₂ reaction between 500 and 600 °C.

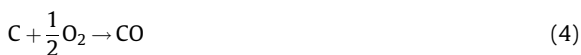
The CO₂/CO ratio during the C–NO₂–O₂ reaction was also evaluated. The obtained values were higher in the presence of water (5.1 at 300 °C to 1.1 at 600 °C) compared to those obtained in the absence of water (4 at 300 °C to 0.9) at 600 °C.

In order to develop the kinetic model, the influence of the main oxidant concentration was also performed. Hence, it was observed that the rate of carbon consumption as well as the rates of CO and CO₂ formation increases linearly with the increase of the NO₂ inlet mole fraction at a given temperature. Such results prove that the reaction order with respect to NO₂ may be close to one.

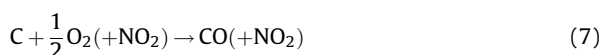
In addition, for a fixed NO₂ mole fraction (~ 400 ppm), the increase of O₂ concentration, at two different temperatures, 300 °C and 400 °C, resulted in an increase of the rate of carbon consumption. These results are taken into account to determine the reaction order with respect to O₂.

Furthermore, for a NO₂ mole fraction of ~ 400 ppm and 5 % O₂, at 300 °C, the increase of the water vapour inlet mole fraction (0 to 10 %) leads to the increase of the rate of carbon consumption. These experiments are used to determine the reaction order with respect to H₂O. The obtained results in the previous and current investigations show that the oxidation mechanism of carbon by NO₂ and O₂ comprises two main simultaneous reactions [9–11]:

- a direct reaction between carbon and NO₂ or O₂:



- a cooperative reaction involving simultaneously NO₂ and O₂:



In the above mechanism, it is not assumed that CO₂ could be obtained by CO oxidation by O₂ since some authors [4] found that, during soot combustion, CO₂ is formed on different sites than those of CO.

In addition, it was proven that H₂O exerts a catalytic effect on the direct oxidation of carbon by NO₂ [9–11]. A beneficial effect of H₂O on the direct reaction between carbon and O₂ is also observed in the present study. Both

H₂O catalytic effects on C–NO₂ and C–O₂ reactions are taken into account in this work.

Recent investigations of soot oxidation by simulated diesel exhaust emissions using thermogravimetric analysis confirmed the proposed mechanism [37]. In fact, Lee et al. have noted a lower temperature zone for soot oxidation ranging from 288 to 500 °C and a higher temperature zone ranging from 516 to 626 °C [37].

3.1. Kinetics of Soot-NO₂ reaction

From Eqs. (2) and (3), the following equation has been used to derive the kinetic parameters of soot oxidation:

$$r_{\text{dirNO}_2} (\text{s}^{-1}) = k_{\text{CO}}(T)X_{\text{NO}_2}^m + k_{\text{CO}_2}(T)X_{\text{NO}_2}^n \quad (8)$$

$k_{\text{CO}}(T)$ and $k_{\text{CO}_2}(T)$ are the kinetic constants for the reactions (2) and (3) respectively. X_{NO_2} is the mole fraction of NO₂. The reaction order with respect to NO₂ was taken, as obtained previously, equal to 1 [9–11], thus $m = n = 1$.

The dependence of the different intrinsic rate constants on temperature is expressed by the Arrhenius function (s^{-1}):

$$k = A \cdot \exp\left(-\frac{E_a}{RT}\right) \quad (9)$$

in which A and E_a are the pre-exponential factor and the activation energy, respectively, and R is the molar gas constant (8.314 J mol⁻¹·K⁻¹).

The values of A and E_a are extracted using the previously developed monodimensional model [9–11] of soot oxidation, in which consumption of NO₂ through the soot bed was taken into account. Therefore, the soot bed is split into small layers and the specific oxidation rate is determined by computing for each elementary layer of the fixed bed, the specific oxidation rate and the depletion of NO₂. The specific oxidation rate was obtained by summing the different rates in each layer and comparing this value with the experimental one. The main features of the modelling procedure are given in previous investigations [9–11].

Experiments in the temperature range of 300–600 °C allowed us to describe the temperature dependence of kinetic constants k_{CO} and k_{CO_2} by an Arrhenius function (see Fig. 3):

$$k_{\text{CO}} = 2.44 \times 10^3 \cdot \exp\left(-\frac{66387}{RT}\right) (\text{s}^{-1}) \quad (10)$$

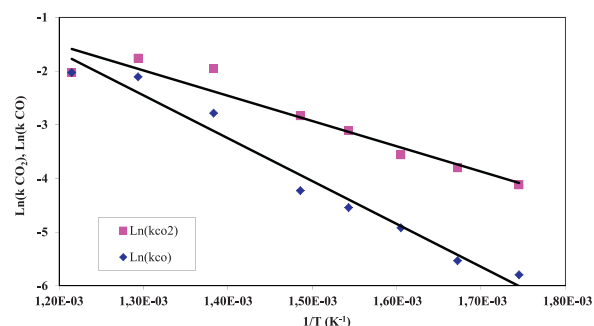


Fig. 3. (Colour online) Arrhenius plot of the kinetic constants of soot-NO₂ reaction.

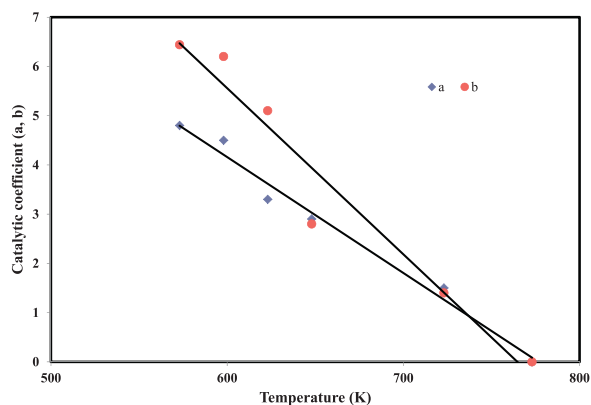


Fig. 4. (Colour online) Evolution of water catalytic coefficients with temperature.

$$k_{\text{CO}_2} = 62.2 \cdot \exp\left(-\frac{39142}{RT}\right) (\text{s}^{-1}) \quad (11)$$

The obtained values for activation energies for soot–NO₂ reactions were not affected by the conversion rate. These values are very close to the activation energies reported by other authors for the oxidation of soot by NO₂. In particular, Lur'e and Mikhno mentioned an activation energy of 50 kJ·mol⁻¹ for graphitized soot oxidation by X_{NO₂} = 0.38–4.5 % in the 373–628 K temperature range [22]. Jacquot et al. reported 46–59 kJ·mol⁻¹ for carbon black oxidation in the presence of X_{NO₂} = 246–437 ppm and a temperature range of 573–723 K [9]. Kandyas et al. obtained an activation energy of 40 kJ·mol⁻¹ for diesel soot oxidation by NO₂ [39]. In recent studies, Tighe et al. [16] as well as Leistner et al. [24] also found energy activation values for C–NO₂ oxidation of the same order of magnitude.

3.2. Kinetics of soot–NO₂–H₂O reaction

Although water vapour is a major component in the automotive exhaust gas, its effect is not well examined in the literature. Previous investigations have mentioned that water vapour exerts a catalytic effect on the oxidation of soot by NO₂ in the presence of oxygen [9]. Jeguirim et al. have proved that the catalytic effect of water affects only the direct C–NO₂ reaction – Eqs. (2) and (3) – and does not affect the cooperative reaction – Eqs. (6) and (7) – [10]. The catalytic effect of H₂O is attributed to the intermediate formation of traces of nitric and nitrous acids, which enhance the rate of carbon oxidation without modifying the global reaction mechanism [12]. The present study shows that the effect of water on the direct C–NO₂ reaction decreases when temperature increases. Such a behaviour should be taken into consideration for the developed kinetic model. Hence, additional terms (1 + a(T)X_{H₂O}^α) and (1 + b(T)X_{H₂O}^β) are introduced in the expressions of the oxidation rate of soot by NO₂ to take into account the catalytic effect of water. The expression of the soot

oxidation rate by NO₂ in the presence of water vapour is expressed by:

$$r_{\text{dirNO}_2, \text{H}_2\text{O}} (\text{s}^{-1}) = k_{\text{CO}}(T)X_{\text{NO}_2} \left(1 + b(T)X_{\text{H}_2\text{O}}^\beta\right) + k_{\text{CO}_2}(T)X_{\text{NO}_2} \left(1 + a(T)X_{\text{H}_2\text{O}}^\alpha\right) \quad (12)$$

k_{CO}(T) and k_{CO₂}(T) are the kinetic constants for the reactions (2) and (3) obtained previously in the absence of water. X_{NO₂} is the mole fraction of NO₂, X_{H₂O} is the mole fraction of water, β and α are the reaction order with respect to H₂O for Eqs. (2) and (3), b(T) and a(T) are the coefficients of the catalytic effect of water of Eqs. (2) and (3), respectively. These coefficients depend on temperature. The reaction orders as well as the catalytic coefficients are determined using the developed kinetic models from the experiments of soot oxidation by NO₂ in the presence of water using the expressions of k_{CO}(T) and k_{CO₂}(T) obtained previously in the absence of water. Hence, the values for the catalytic coefficients are determined at different temperatures. The variations of a and b coefficients with temperature are shown in Fig. 4. The fitting was done with the CO, CO₂, NO and NO₂ emission curves obtained at each temperature.

The best fit was obtained for:

$$a(T) = 18.25 - 0.024 T; T(\text{K}) \quad (13)$$

$$b(T) = 25.92 - 0.034 T; T(\text{K}) \quad (14)$$

$$\alpha = 0.4$$

$$\beta = 0.6$$

3.3. Kinetics of soot–O₂ reaction

The oxidation of soot by oxygen starts at a much higher temperature, around 450 °C (Fig. 2), compared to NO₂, and becomes very fast at 600 °C. Several papers have examined the direct oxidation of soot by oxygen [8,40]. This oxidation is characterized by a direct reaction between oxygen and carbon:



As for NO₂, the oxidation rate r_{dirO_2} can be written as:

$$r_{\text{dirO}_2} (\text{s}^{-1}) = k'_{\text{CO}}(T)X_{\text{O}_2} + k'_{\text{CO}_2}(T)X_{\text{O}_2} \quad (15)$$

k'_{CO}(T) and k'_{CO₂}(T) are the kinetic constants for reactions (4) and (5), respectively. X_{O₂} is the molar fraction of O₂. Based on the values found in the literature, the reaction order with respect to O₂ was taken equal to 1 [8,41].

Experiments in the temperature range of 450 to 600 °C, those of soot oxidation by oxygen, allowed us to describe the temperature dependence of kinetic constants k'_{CO} and k'_{CO₂} by an Arrhenius function as:

$$k'_{\text{CO}} = 3.71 \times 10^7 \cdot \exp\left(-\frac{169198}{RT}\right) (\text{s}^{-1}) \quad (16)$$

$$k'_{\text{CO}_2} = 9.27 \times 10^4 \cdot \exp\left(-\frac{126764}{RT}\right) (\text{s}^{-1}) \quad (17)$$

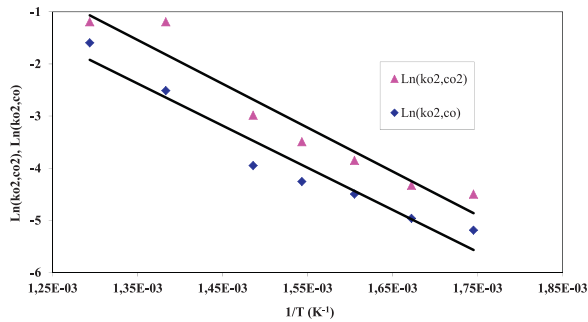


Fig. 5. (Colour online) Arrhenius plot of the kinetic constants for the cooperative reactions.

The obtained activation energy values are quite close to the ones reported by other researchers: Neeft et al. calculated $E_a = 168 \text{ kJ}\cdot\text{mol}^{-1}$ for the oxidation of soot by 10 % O_2 in a temperature range of 442–527 °C [8]. Yezerets et al. reported $E_a = 137 \text{ kJ}\cdot\text{mol}^{-1}$ for soot oxidation with an oxygen concentration of 3–25 % and temperatures ranging from 400 to 550 °C [39,40]. Recently, Lee et al. reported an activation energy close to $155 \text{ kJ}\cdot\text{mol}^{-1}$ for the soot oxidation by simulated diesel exhaust emissions in the temperature range 516–626 °C [37]. Wang–Hansen et al. mentioned an activation energy of $157 \text{ kJ}\cdot\text{mol}^{-1}$ during their kinetic analysis of O_2 -based oxidation of synthetic soot [42]. Leistner et al. obtained $E_a = 164 \text{ kJ}\cdot\text{mol}^{-1}$ for the reaction leading to the emission of CO – Eq. (4) – and $E_a = 147 \text{ kJ}\cdot\text{mol}^{-1}$ for the reaction leading to the emission of CO_2 – Eq. (5) – [24].

3.4. Kinetics of soot– O_2 – H_2O reaction

Experiments of soot oxidation by oxygen performed in the presence of water show a beneficial effect of the presence of water on the oxidation rate. Such a behaviour was previously observed by Ahlström and Odenbrand during the investigation of the combustion characteristics of soot deposits from diesel-powered engines in the presence of 2–10 % O_2 and 0 or 7 % H_2O [43]. Such a behaviour should be taken into account for the developed kinetic model. Hence, the additional term $(1 + c(T)X_{\text{H}_2\text{O}}^\gamma)$ is introduced in the expression of the oxidation rate of soot by O_2 to take into account the beneficial effect of water:

$$r_{\text{dirO}_2, \text{H}_2\text{O}}(s^{-1}) = (k'_{\text{CO}}(T)X_{\text{O}_2} + k'_{\text{CO}_2}(T)X_{\text{O}_2}) \left(1 + c(T)X_{\text{H}_2\text{O}}^\gamma\right) \quad (18)$$

$k'_{\text{CO}}(T)$ and $k'_{\text{CO}_2}(T)$ are the kinetic constants for reactions (4) and (5) obtained previously in the absence of water, γ is the reaction order with respect to H_2O for Eqs. (4) and (5). The reaction orders as well as the catalytic coefficient are determined using the developed kinetic models from the experiments of soot oxidation by O_2 in the presence of water using the expressions of $k'_{\text{CO}}(T)$ and $k'_{\text{CO}_2}(T)$ obtained previously in the absence of water. The fitting was performed on the experimental CO and CO_2 emission

Table 2

Kinetic parameters for soot oxidation by NO_2 , O_2 and H_2O .

α	0.4
β	0.6
γ	0.2
$a(T); T(K)$	$18.25 - 0.024 T$
$b(T); T(K)$	$25.92 - 0.034 T$
$c(T)$	0.3
$k_{\text{CO}_2}(T); (s^{-1})$	$62.2 \cdot \exp\left(-\frac{39142}{RT}\right)$
$k_{\text{CO}}(T); (s^{-1})$	$2.44 \times 10^3 \cdot \exp\left(-\frac{66387}{RT}\right)$
$k'_{\text{CO}}(T); (s^{-1})$	$3.71 \times 10^7 \cdot \exp\left(-\frac{169198}{RT}\right)$
$k'_{\text{CO}_2}(T); (s^{-1})$	$9.27 \times 10^4 \cdot \exp\left(-\frac{126764}{RT}\right)$
$k_{\text{O}_2, \text{CO}}(T); (s^{-1})$	$5.04 \times 10^3 \cdot \exp\left(-\frac{67152}{RT}\right)$
$k_{\text{O}_2, \text{CO}_2}(T); (s^{-1})$	$1.79 \times 10^4 \cdot \exp\left(-\frac{69842}{RT}\right)$

curves at the different studied temperatures. The best fit was obtained for:

$$c(T) = 0.3$$

$$\gamma = 0.2$$

3.5. Kinetics of soot– NO_2 – O_2 reaction

During the oxidation of soot by NO_2 and O_2 between 300 and 600 °C, three reactions occur simultaneously: the direct oxidation of soot by NO_2 , the direct oxidation of soot by O_2 and the cooperative reaction involving a synergetic effect of oxygen and NO_2 . However, the contribution of each reaction on the global oxidation rate depends on temperature. Hence, the following equation may be used to derive the kinetic parameters of the oxidation of soot by NO_2 and O_2 :

$$r(s^{-1}) = r_{\text{dirNO}_2} + r_{\text{dirO}_2} + r_{\text{coop}} \quad (19)$$

where

$$r_{\text{dirNO}_2}(s^{-1}) = k_{\text{CO}}(T)X_{\text{NO}_2} + k_{\text{CO}_2}(T)X_{\text{NO}_2} \quad (20)$$

$$r_{\text{dirO}_2}(s^{-1}) = k'_{\text{CO}}(T)X_{\text{O}_2} + k'_{\text{CO}_2}(T)X_{\text{O}_2} \quad (21)$$

$$r_{\text{coop}}(s^{-1}) = (k_{\text{O}_2, \text{CO}}(T) + k_{\text{O}_2, \text{CO}_2}(T))X_{\text{O}_2}^{0.3}X_{\text{NO}_2} \quad (22)$$

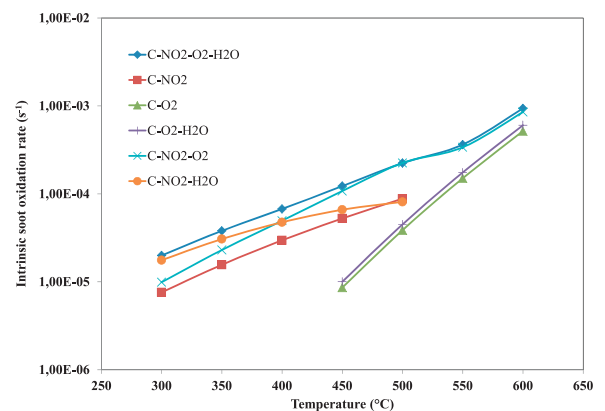


Fig. 6. (Colour online) Comparison between the calculated intrinsic oxidation rates of soot oxidation.

The kinetic parameters for the cooperative reaction were obtained from the experiments of soot oxidation by NO_2 and O_2 taking into account the occurrence of the direct C– NO_2 and direct C– O_2 reactions. The cooperative reaction rate was calculated by subtracting from the global oxidation rate (r) the rate of the direct reaction C– NO_2 (r_{dirNO_2}). The value of 0.3 was found for the reaction order with respect to O_2 by plotting the variation of the logarithm of this rate versus logarithm of oxygen concentrations [11]. Hence, the values of A and E_a for the kinetic constants $k_{\text{O}_2\text{CO}}(T)$ and $k_{\text{O}_2\text{CO}_2}(T)$ are extracted from the developed monodimensional model with the use of the calculated values of the kinetic constants for the direct reactions. The obtained results allowed us to describe the temperature dependence of kinetic constants $k_{\text{O}_2\text{CO}}$ and $k_{\text{O}_2\text{CO}_2}$ by an Arrhenius function such as (see Fig. 5):

$$k_{\text{O}_2\text{CO}} = 5.04 \times 10^3 \cdot \exp\left(-\frac{67152}{RT}\right) (\text{s}^{-1}) \quad (23)$$

$$k_{\text{O}_2\text{CO}_2} = 1.79 \times 10^4 \cdot \exp\left(-\frac{69842}{RT}\right) (\text{s}^{-1}) \quad (24)$$

The obtained activation energy values are very close to the values (60–80 $\text{kJ}\cdot\text{mol}^{-1}$) defined by Messerer et al. for the overall process of adsorption and reaction during the oxidation of soot by NO_2 and O_2 [17]. Leistner et al. obtained 70 $\text{kJ}\cdot\text{mol}^{-1}$ for the reaction involving the decomposition of C(ONO_2) complexes into CO_2 and NO [24].

3.6. Kinetics of soot- NO_2 - O_2 - H_2O reaction

During the oxidation of soot by a mixture containing oxygen, nitrogen dioxide and water vapour, it was shown that the direct C– NO_2 and C– O_2 reactions and the cooperative C– NO_2 - O_2 reaction occur simultaneously. Water vapour has a catalytic effect on both direct reactions but does not significantly influence the cooperative reaction (Fig. 2). Hence, the global oxidation rate of soot oxidation by diesel exhaust emission may be expressed by:

$$\begin{aligned} r(\text{s}^{-1}) = & k_{\text{CO}_2}(T)P_{\text{NO}_2} \left(1 + a(T)X_{\text{H}_2\text{O}}^\alpha\right) \\ & + k_{\text{CO}}(T)P_{\text{NO}_2} \left(1 + b(T)X_{\text{H}_2\text{O}}^\beta\right) \\ & + \left(k'_{\text{CO}}(T)X_{\text{O}_2} + k'_{\text{CO}_2}(T)X_{\text{O}_2}\right) \\ & + \left(1 + c(T)X_{\text{H}_2\text{O}}^\gamma\right) \\ & + (k_{\text{O}_2\text{CO}}(T) + k_{\text{O}_2\text{CO}_2}(T))X_{\text{O}_2}^{0.3}X_{\text{NO}_2} \end{aligned} \quad (25)$$

The obtained values of the different kinetic parameters were determined previously for each reaction and are summarized in Table 2. Using the obtained kinetic constants, the intrinsic soot oxidation rates for the different reactions are calculated for a gas mixture containing 400 ppm NO_2 , 10 % O_2 and 5 % H_2O at a temperature range from 300 to 600 °C. The obtained values are compared in Fig. 6.

Fig. 6 shows that the calculated intrinsic oxidation rates confirm the role of each component from the exhaust gas on the mechanism of soot oxidation in diesel exhaust emissions. Hence, from 300 to 450 °C, the direct oxidation of soot by NO_2 and the cooperative C– NO_2 - O_2 reaction are responsible for soot oxidation. In this temperature range, water vapour has a catalytic effect on the direct C– NO_2 . Above 450 °C, the direct oxidation of soot by O_2 starts and becomes the dominant reaction above 600 °C. The addition of water vapour leads to a slight increase of the oxidation rate of soot by oxygen.

The above equations were also verified for the different inlet NO_2 , O_2 and H_2O concentrations used. The as-obtained calculated rates of soot consumption were in good agreement with the experimental ones. This agreement tends to be better as the rate of consumption decreases. However, the mean standard deviation is equal to 10 %.

4. Conclusion

Carbon black was used as a model for diesel soot and was oxidized under modern diesel engine emission conditions, 300–600 °C, NO_2 (0–400 ppm), O_2 (0–10 %) and H_2O (0–10 %), in a fixed bed reactor. The gases issued from combustion were exclusively CO , CO_2 and NO .

It was found that carbon is mainly oxidised by NO_2 at 300–450 °C and by O_2 at 450–600 °C, and that water has a catalytic effect on these reactions, called direct reactions. Moreover, in the presence of both NO_2 and O_2 , the oxidation rate was enhanced, compared to both direct reactions, without the catalytic effect of water.

According to experimental data, a kinetic mechanism was established and then a mathematical one-dimensional fixed bed model was proposed. Kinetic constants for each identified reaction were determined by the data fitting of the theoretical CO and CO_2 emission curves with the experimental ones. The kinetic constants have shown an Arrhenius behaviour. Moreover, constants related to the water catalytic effect were also determined by modelling.

The comparison between the experimental oxidation rates and the ones obtained by the kinetic constants extracted by modelling shows a good agreement between the experimental data and the kinetic mechanism proposed.

This study contributes to the investigation of the oxidation mechanism of diesel soot in real conditions. Some further investigations should be done, such as the influence of mass carbon conversion on the overall combustion process, before proposing a set of kinetic constants to car manufacturers in order for them to predict the behaviour of the diesel filter particulate regeneration.

Acknowledgements

M. Labaki would like to thank the “Agence universitaire de la Francophonie (AUF) – Région du Moyen-Orient”, for financial support. The authors are also grateful to Mrs Damaris Kehrlé and Nelly Dawson for carrying out some experiments. The authors would like to thank the Laboratoire “Gestion des risques et environnement” for technical support.

References

- [1] M. Jeguirim, V. Tschamber, J.F. Brilhac, P. Ehrburger, *J. Anal. Appl. Pyrolysis* 72 (2004) 171–181.
- [2] X. Gao, S. Liu, Y. Zhang, Z. Luo, M. Ni, K. Cen, *Fuel Process. Technol.* 92 (2011) 139–146.
- [3] H. Muckenhuber, H. Grothe, *Carbon* 44 (2006) 546–559.
- [4] Z. Du, A.F. Sarofim, J.P. Longwell, C.A. Mims, *Energy Fuels* 5 (1991) 214–221.
- [5] W. He, R. He, T. Ito, T. Suda, J. Sato, *Combust. Sci. Technol.* 183 (2011) 868–882.
- [6] M.J. Biggs, P.K. Agarwal, *Chem. Eng. Sci.* 52 (1997) 941–952.
- [7] J.K. Floess, J.P. Longwell, A.F. Sarofim, *Energy Fuels* 2 (1988) 18–26.
- [8] J.P.A. Neef, T. Xander Nijhuis, E. Smakman, M. Makkee, J.A. Moulijn, *Fuel* 76 (1997) 1129–1136.
- [9] F. Jacquot, V. Logie, J.F. Brilhac, P. Gilot, *Carbon* 40 (2002) 335–343.
- [10] M. Jeguirim, V. Tschamber, J.F. Brilhac, P. Ehrburger, *Fuel* 84 (2005) 1949–1956.
- [11] M. Jeguirim, V. Tschamber, J.F. Brilhac, *J. Chem. Technol. Biotechnol.* 84 (2009) 770–776.
- [12] M. Jeguirim, V. Tschamber, J.F. Brilhac, *Int. J. Chem. Kinet.* 41 (2009) 236–244.
- [13] J. Jung, J.H. Lee, S. Song, K.M. Chun, *Int. J. Automot. Technol.* 9 (2008) 423–428.
- [14] M. Schejbal, J. Štěpánek, M. Marek, P. Kočí, M. Kubíček, *Fuel* 89 (2010) 2365–2375.
- [15] A. Setiabudi, M. Makkee, J.A. Moulijn, *Appl. Catal. B* 50 (2004) 185–194.
- [16] C.J. Tighe, M.V. Twigg, A.N. Hayhurst, J.S. Dennis, *Combust. Flame* 159 (2012) 77–90.
- [17] A. Messerer, R. Niessner, U. Pöschl, *Carbon* 44 (2006) 307–324.
- [18] J. Kleffmann, K.H. Becker, M. Lackhoff, P. Wiesen, *Phys. Chem. Chem. Phys.* 1 (1999) 5443–5450.
- [19] F. Arens, L. Gutzwiller, U. Baltensperger, H.W. Gaggeler, M. Ammann, *Environ. Sci. Technol.* 35 (2001) 2191–2199.
- [20] A. Pashkova, S. Seisel, *Z. Phys. Chem.* 224 (2010) 1205–1217.
- [21] A.P. Prince, J.L. Wade, V.H. Grassian, P.D. Kleiber, M.A. Young, *Atmos. Environ.* 36 (2002) 5729–5740.
- [22] B.A. Lur'e, A.V. Mikhno, *Kinet. Catal.* 38 (1997) 490–497.
- [23] P.G. Gray, D.D. Do, *Chem. Eng. Commun.* 117 (1992) 219–240.
- [24] K. Leistner, A. Nicolle, P. Da Costa, *J. Phys. Chem. C* 116 (2012) 4642–4654.
- [25] A. Raj, Z. Zainuddin, M. Sander, M. Kraft, *Carbon* 49 (2011) 1516–1531.
- [26] R. López-Fonseca, I. Landa, U. Elizundia, M.A. Gutiérrez-Ortiz, J.R. González-Velasco, *Combust. Flame* 144 (2006) 398–406.
- [27] N. Zouaoui, J.F. Brilhac, F. Mechat, M. Jeguirim, B. Djellouli, P. Gilot, *J. Thermal Anal. Calorim.* 102 (2010) 837–849.
- [28] M. Kalogirou, Z. Samaras, *J. Thermal Anal. Calorimetry* 98 (2009) 215–224.
- [29] J. Song, C.H. Jeon, A.L. Boehman, *Energy Fuels* 24 (2010) 2418–2428.
- [30] M. Jeguirim, K. Villani, J.F. Brilhac, J.A. Martens, *Appl. Catal. B* 96 (2010) 34–40.
- [31] M. Kalogirou, D. Katsaounis, G. Koltsakis, Z. Samaras, *Top. Catal.* 42–43 (2007) 247–251.
- [32] M. Issa, C. Petit, A. Brillard, J.F. Brilhac, *Fuel* 87 (2008) 740–750.
- [33] M. Issa, H. Mahzoul, A. Brillard, J.F. Brilhac, *Chem. Eng. Technol.* 32 (2009) 1859–1865.
- [34] Z. Zhang, Y. Zhang, Q. Su, Z. Wang, Q. Li, X. Gao, *Environ. Sci. Technol.* 44 (2010) 8254–8258.
- [35] B. Azambre, S. Collura, P. Darcy, J.M. Trichard, P. Da Costa, A. García-García, A. Bueno-López, *Fuel Process. Technol.* 92 (2011) 363–371.
- [36] K. Leistner, A. Nicolle, P. Da Costa, *Energy Fuels* 26 (2012) 6091–6097.
- [37] K.O. Lee, H. Seong, S.M. Choi, *Proc. Combust. Inst.* 34 (2013) 3057–3065.
- [38] S.J. Jelles, R.R. Krul, M. Makkee, J.A. Moulijn, *Catal. Today* 53 (1999) 623–630.
- [39] I.P. Kandyas, O.A. Haralampous, G.C. Koltsakis, *Ind. Eng. Chem. Res.* 41 (2002) 5372–5384.
- [40] A. Yezerets, N.W. Currier, D.H. Kim, H.A. Eadler, W.S. Epling, C.H.F. Peden, *Appl. Catal. B* 61 (2005) 120–129.
- [41] T. JunShi, S. Qiang, H. BaiLei, Y. Qiang, *Sci. China E Technol. Sci.* 52 (2009) 1535–1542.
- [42] C. Wang–Hansen, S. Soltani, B. Andersson, *J. Phys. Chem. C* 117 (2013) 522–531.
- [43] A.F. Ahlström, C.U.I. Odenbrand, *Carbon* 27 (1989) 475–483.